*Kovove Mater.* 49 2011 17–22
*DOI: 10.4149/km_2011_1_17*

# Formation of two amorphous phases in the $Ni_{60}Nb_{18}Y_{22}$ alloy after high pressure torsion

B. B. Straumal[1,2,4]*, A. A. Mazilkin[1,2], S. G. Protasova[1,2], D. Goll[2,3], B. Baretzky[4], A. S. Bakai[5], S. V. Dobatkin[6]

[1] *Institute of Solid State Physics, Russian Academy of Sciences, 142432 Chernogolovka, Moscow district, Russia*
[2] *Max-Planck-Institut für Metallforschung, Heisenbergstraße 3, 70569 Stuttgart, Germany*
[3] *Hochschule Aalen, Beethovenstraße 1, D-73430 Aalen, Germany*
[4] *Karlsruher Institut für Technologie (KIT), Institut für Nanotechnologie, Hermann-von-Helmholtz-Platz 1, 76344 Eggenstein-Leopoldshafen, Germany*
[5] *NSC Kharkiv Institute of Physics and Technology, Akademichna st. 1, Kharkiv 61108, Ukraine*
[6] *A. A. Baikov Institute of Metallurgy and Materials Science, RAS, Leninsky prosp. 49, 117991 Moscow, Russia*

Received 24 July 2010, received in revised form 28 August 2010, accepted 30 August 2010

## Abstract

It has been demonstrated for the first time that severe plastic deformation (SPD) permits to produce the metallic alloys containing two coexisting amorphous phases from the crystalline multiphase alloy. The as-cast $Ni_{60}Nb_{18}Y_{22}$ alloy was coarse-grained and contained mainly NiY phase (grain size 25 μm) and also $NbNi_3$, $Ni_2Y$, $Ni_7Y_2$ and $Ni_3Y$ phases (grain size 3–5 μm). High pressure torsion (4 GPa, 10 torsions) completely changed the structure. The sample after SPD contained two glassy phases and two other nanocrystalline NiY and $Nb_{15}Ni_2$ phases (grain size about 20 nm). The coarse-grained alloy was mainly ferromagnetic with a small paramagnetic component. After SPD the alloy becomes strongly diamagnetic with a small ferromagnetic component. Therefore, it has been revealed that severe plastic deformation allows one to produce the composite amorphous alloys.

Key words: severe plastic deformation, Y-Ni-Nb alloys, amorphous phases

## 1. Introduction

It is well known that the quenching from liquid state permits to synthesize the amorphous state (metallic glass) [1–3]. Recently the multicomponent alloys were discovered whose quenching from the melt permitted to produce simultaneously two coexisting amorphous phases. The first phase-separated metallic glass was probably prepared in the Zr-Y-Al-Ni system by Inoue et al. in 1994 [4]. In 2004, Kündig et al. obtained the two-phase amorphous alloys in the Zr-La-Al-Ni-Cu system [5]. Later the phase-separated metallic glasses were manufactured in several alloy systems: Ni-Nb-Y [6–13], (Ti, Zr)-Y-Al-Co [14–16], Cu-(Zr, Hf)-(Gd, Y)-Al [17], Nd-Zr-Al-Co [18], Zr-(Cu, Ce, Pr, Nd)-Al-(Ni, Ag) [3, 19, 20]. In these materials the decomposition and structure formation take place already in the melt prior to solidification. These alloys have exotic properties such as extraordinary plasticity [17, 21] and may be extremely interesting for various applications [1, 10, 22]. Therefore, it is important to find other methods for the synthesis of metallic glasses containing simultaneously two (or more) different amorphous phases.

The Ni-Nb-Y system has been chosen for the experiments. It has been shown that the miscibility gap of the monotectic binary Nb-Y system extends into the ternary Ni-Nb-Y system up to 70 at.% Ni as a consequence of the positive mixing enthalpy between Nb and Y [7]. The experimental evidence of phase separation in the melt of $Ni_{58.5}Nb_{20.25}Y_{21.25}$ (numbers indicate at.%) was obtained by in situ X-ray diffraction at elevated temperatures and differential scanning calorimetry [6–9]. The melt in this alloy separated in two immiscible liquid phases $Ni_{58.5}Nb_{20.25}Y_{21.25}$ and $Ni_{58}Nb_{10.1}Y_{30.9}$ already before quenching. The quick

---

*Corresponding author: tel.: +7 49652 22957; fax: +7 49652 49701; e-mail address: straumal@issp.ac.ru[1]; straumal@mf.mpg.de[2]

cooling of this mixture leads to the formation of two amorphous metallic phases from two pre-existing liquid phases [6–9]. The microstructure consisted of two amorphous regions, one Nb-enriched and the other Y-enriched, with a size distribution from several nanometres up to micrometer-dimension.

Severe plastic deformation of crystalline alloys also permits to transform them into amorphous phase [23–27]. The goal of this work is to try to obtain the coexisting amorphous phases by the high pressure torsion (HPT). In our case we would try to obtain two coexisting amorphous phases not from two coexisting liquids (or from one amorphous phase) but from the mixture of crystalline phases.

## 2. Experimental

The $Ni_{60}Nb_{18}Y_{22}$ (numbers indicate at.%) alloy which was chosen for the investigations is shown by the asterisk in the Y-Ni-Nb phase diagram (Fig. 1a). It is very close to the composition $Ni_{58.5}Nb_{20.25}Y_{21.25}$ studied in [7–9]. The $Ni_{60}Nb_{18}Y_{22}$ alloy was prepared by using high purity components (4N Ni, 3N Nb and 3N Y) for vacuum induction melting. After grinding, sawing and chemical etching, as-cast disks of these alloys, with 3 mm in diameter, were subjected to HPT at room temperature under a pressure of 4 GPa in a Bridgman anvil type unit (10 torsions, duration of process about 300 s). X-ray diffraction (XRD) data were obtained on a Siemens diffractometer (Co K$\alpha$ radiation). Transmission electron microscopy (TEM) investigations were carried out on a JEM-100CX microscope with an accelerating voltage of 100 kV. Scanning electron microscopy (SEM) and electron-probe microanalysis (EPMA) were carried out in a Supra 50VP microscope equipped with a LINK energy-dispersive spectrometer produced by Oxford Instruments. Grain size $D$ was estimated by the Scherrer formula $D = 0.9\lambda/\beta\cos\theta$ (here $\lambda$ is the wavelength, $\beta$ is the physical line broadening and $\theta$ is the diffraction angle) [28]. The magnetic properties were measured on a superconducting quantum interference device SQUID (Quantum Design MPMS-7 and MPMS-XL). The magnetic field was applied parallel to the sample plane (in plane).

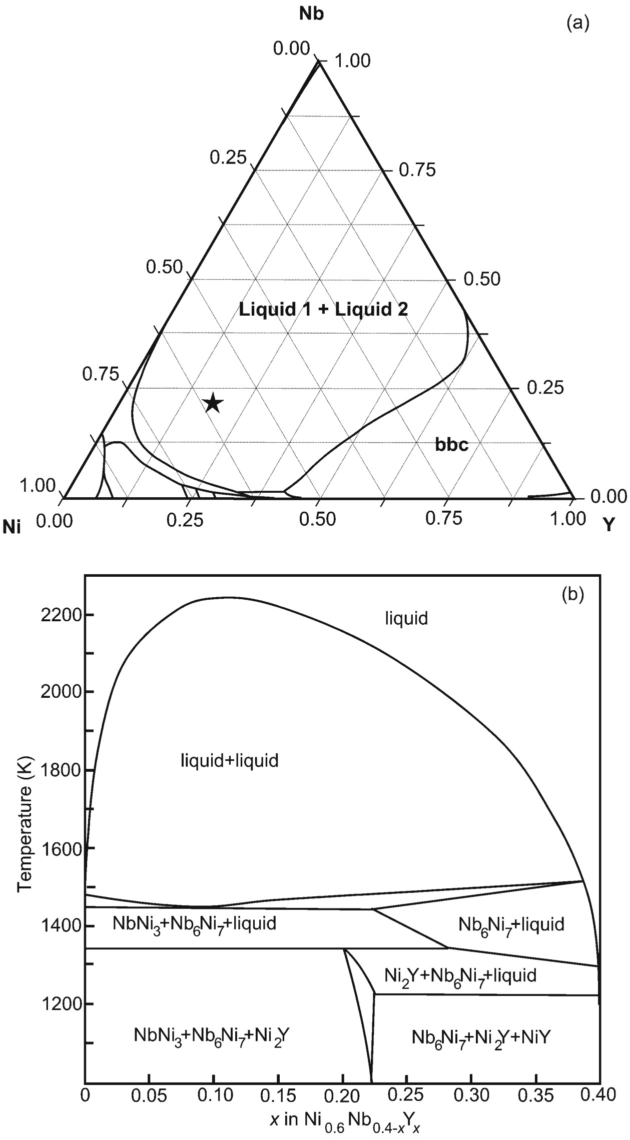

Fig. 1. (a) Liquidus projection obtained by the CALPHAD method of the Y-Ni-Nb ternary phase diagram [31]. The composition of the triple $Ni_{60}Nb_{18}Y_{22}$ alloy chosen for investigations is marked by the asterisk. (b) Calculated pseudo-binary section of the ternary phase diagram $Ni_{60}Y_{40}$-$Ni_{60}Nb_{40}$ [7].

## 3. Results and discussion

The X-rays diffraction spectrum of the $Ni_{60}Nb_{18}Y_{22}$ alloy before deformation is shown in Fig. 2a. The main phase component is the NiY phase. The as-cast sample contains also other crystalline phases. The spectrum is well described by deconvolution into the peaks of the NiY, $NbNi_3$, $Ni_2Y$, $Ni_7Y_2$ and $Ni_3Y$ phases. No input of the amorphous phase(s) was detected. SEM micrograph of the as-cast $Ni_{60}Nb_{18}Y_{22}$ alloy is shown in Fig. 3. The microstructure contains the large spherical grains of the $NbNi_3$ phase (mean grain size is about 25 µm) surrounded by the mixture of NiY, $Ni_2Y$, $Ni_7Y_2$ and $Ni_3Y$ phases (grain size 3–5 µm). In Fig. 1b the calculated pseudo-binary section of the ternary phase diagram $Ni_{60}Y_{40}$-$Ni_{60}Nb_{40}$ is shown [7]. The composition of our alloy is very close to this pseudo-binary section (Fig. 1b) and is nearly in the middle of the horizontal axis. Nevertheless, only the NiY, $NiY_2$ and $NbNi_3$ phases observed in the as-cast sample are present in the pseudo-binary

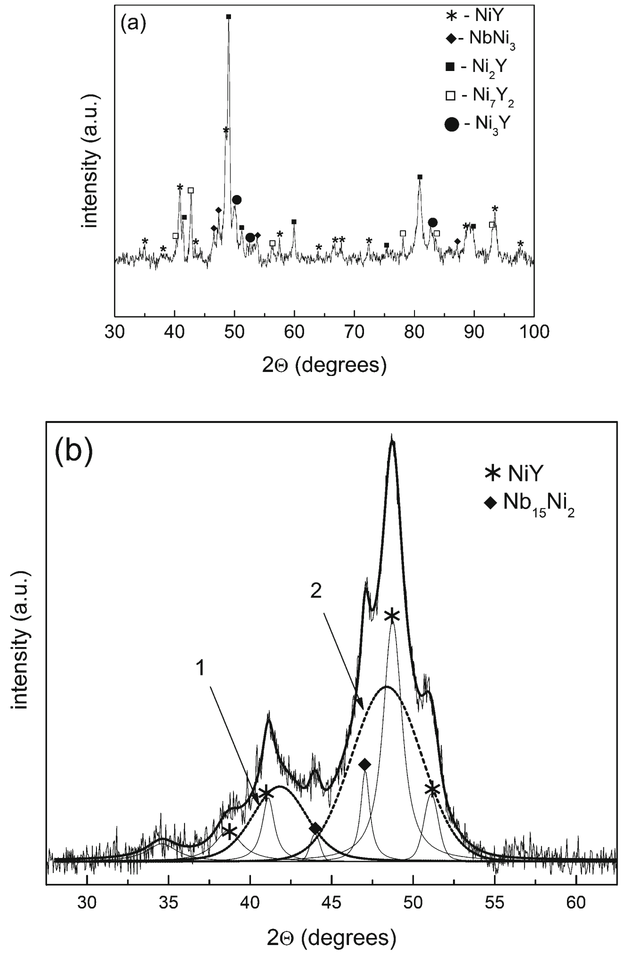

Fig. 2. (a) X-rays diffraction spectrum of the $Ni_{60}Nb_{18}Y_{22}$ alloy before deformation. The main phase component is the NiY phase. Other phases are $NbNi_3$, $Ni_2Y$, $Ni_7Y_2$ and $Ni_3Y$. (b) X-rays diffraction spectrum of the $Ni_{60}Nb_{18}Y_{22}$ alloy after HPT. It consists of two halos from two amorphous phases (1 and 2) which are superimposed over the peaks of crystalline phases NiY and $Nb_{15}Ni_2$.

section (Fig. 1b). Two other phases $Ni_3Y$ and $Ni_7Y_2$ are not represented in the calculated phase diagram (Fig. 1b). And vice versa, the phase $Nb_6Ni_7$ (Fig. 1b) was not observed in the as-cast sample. The coarse-grained alloy was mainly ferromagnetic with a small paramagnetic component (Fig. 4a). It is known that $Ni_3Y$ and $Ni_7Y_2$ phases are ferromagnetic [29, 30]. The information about magnetic properties of other phases in the Y-Ni-Nb system is absent, to the best of our knowledge. Unfortunately, there are only few experimental data on the ternary Y-Ni-Nb phase diagram. The phase diagrams (Fig. 1) were calculated using CALPHAD [7, 31]. In our experiments, as well as in [6–10], no ternary phases were observed. Ternary Y-Ni-Nb phases are also absent in the existing databases [32, 33].

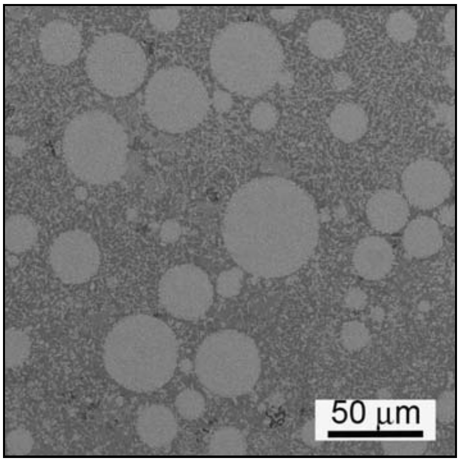

Fig. 3. SEM micrograph of the $Ni_{60}Nb_{18}Y_{22}$ alloy before deformation.

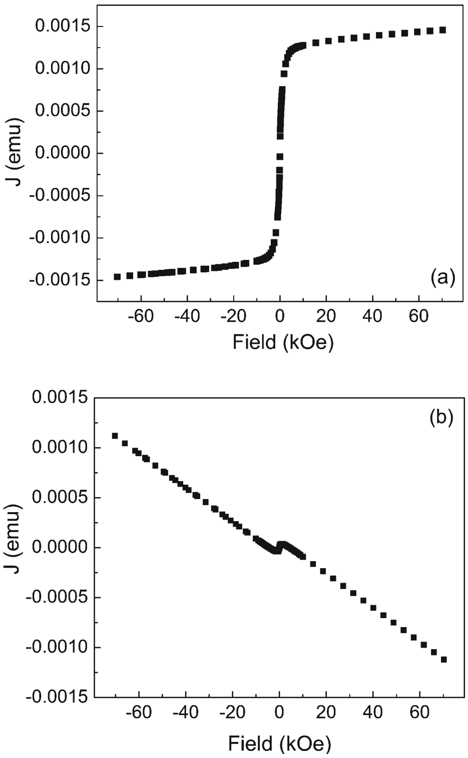

Fig. 4. (a) Magnetization curve of the $Ni_{60}Nb_{18}Y_{22}$ alloy before deformation. It is mainly ferromagnetic with a small paramagnetic component. (b) Magnetization curve of the $Ni_{60}Nb_{18}Y_{22}$ alloy after deformation. It is mainly diamagnetic with a small ferromagnetic component.

High pressure torsion completely changed the structure. The $NbNi_3$, $Ni_2Y$, $Ni_7Y_2$ and $Ni_3Y$ phases present in the starting coarse-grained alloy completely disappeared after HPT. Only NiY crystalline phase which existed in the as-cast state remains after HPT. The respective XRD-pattern is shown in Fig. 3b. It contains the partly superimposed halos of two

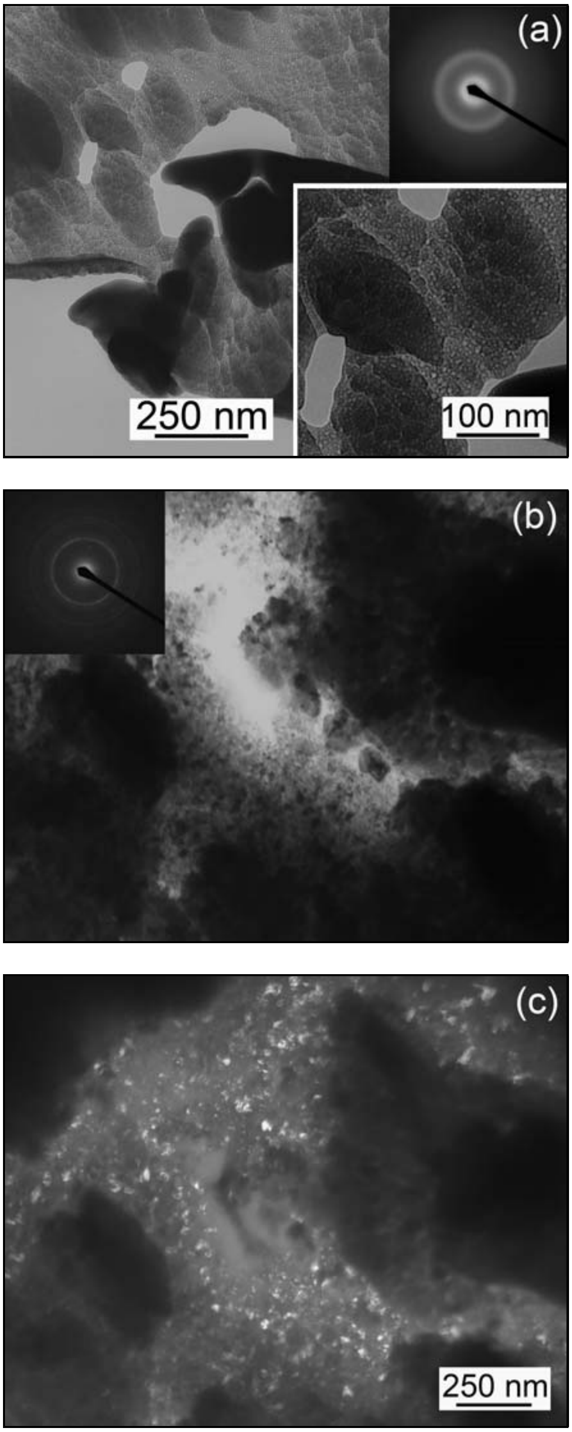

Fig. 5. TEM micrographs of the $Ni_{60}Nb_{18}Y_{22}$ alloy after HPT. (a) Predominantly amorphous area (bright field, insets show enlarged portion of a micrograph and the electron diffraction pattern); (b, c) predominantly crystalline area, (b) bright field, (c) dark field. Inset shows the electron diffraction pattern.

amorphous phases with maxima at $q_1 = 25.1\,\mathrm{nm}^{-1}$ and $q_2 = 28.8\,\mathrm{nm}^{-1}$ and peaks of two other crystalline NiY and $Nb_{15}Ni_2$ phases. It is very close to the halos positions $q_1 = 26.3\,\mathrm{nm}^{-1}$ and $q_2 = 29.5\,\mathrm{nm}^{-1}$ observed in the quenched alloys [7]. The area under scattering curve corresponding to the amorphous phase with $q_2 = 28.8\,\mathrm{nm}^{-1}$ (and also the amount of this phase) is about three times higher than that of the amorphous phase with $q_1 = 25.1\,\mathrm{nm}^{-1}$. The maximum for the larger scattering vector is slightly higher, as in the quenched alloys as well [7]. The calculation of the areas below scattering curves and diffraction maxima for the crystalline phases show that their fraction ratio is about 1 : 1. The peak broadening of the phases permits to estimate their grain size as being about 20 nm. HPT completely changes also magnetic properties of the alloy. Along with remaining ferromagnetism behavior, the strong diamagnetism is observed (Fig. 4b).

In Fig. 5 the TEM micrographs of the sample after HPT are shown. It was possible to obtain the micrographs from the predominantly amorphous (Fig. 5a) and predominantly crystalline (Fig. 5b) areas. Figure 5a shows the bright-field image of the amorphous part of the sample. There are no diffraction rings for the crystalline phases and only one amorphous halo in the selected area electron diffraction (SAED) pattern. Though two halos were observed in XRD spectrum, they cannot be resolved in the SAED pattern due to the lower angular resolution of this method. Nevertheless, the contrast between two different amorphous phases occurs. This contrast is due to the different densities of two amorphous phases. Similar to [7–9], the dark regions are Nb-rich and bright regions are Y-rich, since the atomic weight of niobium is higher than that of yttrium.

The finely mixed layers and grains of two different amorphous phases are visible in the thin areas of the sample. The fine 5–10 nm round bubbles of bright Y-rich amorphous phase are embedded in the darker Nb-rich "grains" (see the inset with higher magnification). These dark grains are slightly elongated and have a 20–200 nm size. The Nb-rich dark grains are in turn separated by the few nm thick layers of the bright Y-rich amorphous phase. This microstructure radically differs from that obtained by the melt spinning [7–9]. The size of the heterogeneities in the phase-separated amorphous metallic alloys obtained by the quenching from the melt ranges from nanometer- to micrometer dimension with the features of self-similarity [6–10]. In other words, the bright phase contains spherical dark regions, and they in turn contain the smaller bright spheres, etc. Such a Russian-matreshka-doll-like structure forms as a result of sequential formation of Nb- and Y-rich phases during the cooling of the melt in the dome-like immiscibility area which broadens with decreasing temperature [7].

In Fig. 5b the bright and dark field images of the crystalline area of the HPT-treated sample are shown. The SAED pattern contains only strong lines of the

NiY phase together with weak $Nb_{15}Ni_2$ reflections and no amorphous halo(s). The size of crystalline grains is about 20 nm and coincides well with the data obtained from the shape of XRD peaks.

The requirements for the formation of a two-phase amorphous metallic alloy are on the one hand a high glass-forming ability, and on the other hand a strong de-mixing tendency of components. Second condition is in the contradiction to high glass-forming ability [2]. In case of quenching from the liquid phase, two amorphous phases form from two liquid phases already separated in the de-mixing area of the phase diagram. In case of the severe plastic deformation the situation is quite different. Due to the high shear deformation, SPD leads to the grain refinement and formation of the nano-grained structure [34, 35]. With increasing deformation the stationary state (and stationary grain size about 100 nm) can be reached when the formation of new defects is compensated by the dynamic recovery [36]. In our case the as-cast material is multiphase, inside the crystalline grains there exist the compositional fluctuations combined with local compositional short-range order. The severe shear during HPT destroys the short-range order in the alloy leading to the formation of the amorphous phase. The possibility of the growth of the amorphous areas by the movement of the amorphization front during SPD was demonstrated in the simulations [37–40]. In the two-phase amorphous metallic alloys the specific microstructure may form during the viscous flow where the "grains" of the more rigid amorphous phase are surrounded by the less rigid ones like in Fig. 5a [41–43]. Therefore, it is demonstrated that severe plastic deformation allows one to produce the composite amorphous alloys. Though HPT permits to produce only rather thin samples, the utilization of another SPD techniques (like for example of the equal-channel angular pressing) would allow to manufacture the bulk amorphous composites.

## 4. Conclusions

We demonstrated for the first time that the severe plastic deformation by high pressure torsion permits to obtain metallic alloys containing simultaneously two different coexisting amorphous phases. The originally ferromagnetic coarse-grained $Ni_{60}Nb_{18}Y_{22}$ alloy becomes almost fully amorphous and diamagnetic (with a small ferromagnetic component). Therefore, it is demonstrated that severe plastic deformation allows one to produce the bulk composite amorphous alloys.

## Acknowledgements

Authors thank the Russian Foundation for Basic Research (contract 09-08-90469) and Ukrainian Fundamental Research State Fund (contract Φ28.2107) for the financial support of investigations and exchange travel. Authors cordially thank Prof. G. Schütz and Dr. E. Goering for stimulating discussions.

## References

[1] LOEFFLER, J. F.—BOSSUYT, S.—GLADE, S. C.—JOHNSON, W. L.—WAGNER, W.— THIYAGARAJAN, P.: Appl. Phys. Lett., *77*, 2000, p. 525. doi:10.1063/1.127032

[2] INOUE, A.—TAKEUCHI, A.: Mater. Trans., *40*, 2002, p. 1892. doi:10.2320/matertrans.43.1892

[3] LOUZGUINE-LUZGIN, D. V.—SEKI, I.—YAMAMOTO, T.—KAWAJI, H.—SURYANARAYANA, C. —INOUE, A.: Phys. Rev. B, *81*, 2010, p. 144202. doi:10.1103/PhysRevB.81.144202

[4] INOUE, A.—CHEN, S.—MASUMOTO, T.: Mater. Sci. Eng. A, *179/180*, 1994, p. 346. doi:10.1016/0921-5093(94)90224-0

[5] KÜNDIG, A. A.—OHNUMA, M.—PING, D. H.—OHKUBO, T.—HONO, K.: Acta Mater., *52*, 2004, p. 2441. doi:10.1016/j.actamat.2004.01.036

[6] MATTERN, N.—KUEHN, U.—GEBERT, A.—GEMMING, T.—ZINKEVICH, M.—WENDROCK, H.—SCHULTZ, L.: Scripta Mater., *53*, 2005, p. 271. doi:10.1016/j.scriptamat.2005.04.018

[7] MATTERN, N.—KÜHN, U.—GEBERT, A.—SCHOEPS, A.—GEMMINGA, T.—SCHULTZ, L.: Mater. Sci. Eng. A, *449/451*, 2007, p. 207. doi:10.1016/j.msea.2006.02.269

[8] MATTERN, N.: J. Non-Cryst. Solids, *353*, 2007, p. 1723. doi:10.1016/j.jnoncrysol.2007.01.042

[9] MATTERN, N.—GEMMING, T.—GOERIGK, G.—ECKERT, J.: Scripta Mater., *57*, 2007, p. 29. doi:10.1016/j.scriptamat.2007.03.016

[10] CONCUSTELL, A.—MATTERN, N.—WENDROCK, H.—KUEHN, U.—GEBERT, A.—ECKERT, J.—GREER, A. L.—SORT, J.—BARO, M. D.: Scripta Mater., *56*, 2007, p. 85. doi:10.1016/j.scriptamat.2006.09.026

[11] MATTERN, N.—ZINKEVICH, M.—LOSER, W.—BEHR, G.—ACKER, J.: J. Phase Equil. Diff., *29*, 2008, p. 141. doi:10.1007/s11669-007-9243-2

[12] MATTERN, N.—GOERIGK, G.—VAINIO, U.—MILLER, M. K.—GEMMING, T.—ECKER, J.: Acta Mater., *57*, 2009, p. 903. doi:10.1016/j.actamat.2008.10.028

[13] MATTERN, N.—GEMMING, T.—THOMAS, J.—GOERIGK, G.—FRANCZ, H.—ECKERT, J.: J. Alloys Comp., *495*, 2010, p. 299. doi:10.1016/j.jallcom.2009.10.013

[14] PARK, B. J.—CHANG, H. J.—KIM, D. H.—KIM, W. T.: Appl. Phys. Lett., *85*, 2004, p. 6353. doi:10.1063/1.1842360

[15] JAYARAJ, J.—PARK, J. M.—GOSTIN, P. F.—FLEURY, E.—GEBERT, A.—SCHULTZ, L.: Intermet., *17*, 2009, p. 1120. doi:10.1016/j.intermet.2009.05.008

[16] PARK, B. J.—SOHN, S. W.—KIM, W. T.—KIM, D. H.: J. Alloys Comp., *483*, 2009, p. 260. doi:10.1016/j.jallcom.2008.08.136

[17] PARK, E. S.—KYEONG, J. S.—KIM, D. H.: Scripta Mater., *57*, 2007, p. 49. doi:10.1016/j.scriptamat.2007.03.008

[18] PARK, E. S.—JEONG, E. Y.—LEE, J.-K.–BAE, J. C.—KWON, A. R.—GEBERT, A.—SCHULTZ, L.—CHANG, H. J.—KIM, D. H.: Scripta Mater., *56*, 2007, p. 197. doi:10.1016/j.scriptamat.2006.10.020

[19] LOUZGUINE-LUZGIN, D. V.—WADA, T.—KATO, H.—PEREPEZKO, J.—INOUE, A.: Intermetall., *18*, 2010, p. 1235. doi:10.1016/j.intermet.2010.03.018

[20] WADA, T.—LOUZGUINE-LUZGIN, D. V.—INOUE, A.: Scripta Mater., *57*, 2007, p. 901. doi:10.1016/j.scriptamat.2007.07.032

[21] LEE, S.-C.—HUH, M.-Y.—KIM, H.-J.—LEE, J.-C.: Mater. Sci. Eng. A, *485*, 2008, p. 61. doi:10.1016/j.msea.2007.08.068

[22] KHADEMIAN, N.—GHOLAMIPOUR, R.: Mater. Sci. Eng. A, *527*, 2010, p. 3079. doi:10.1016/j.msea.2010.01.086

[23] PROKOSHKIN, S. D.—KHMELEVSKAYA, I. Y.—DOBATKIN, S. V.—TRUBITSYNA, I. B.—TAT'YANIN, E. V.—STOLYAROV, V. V.—PROKOF'EV, E. A.: Phys. Metals Metallogr., *97*, 2004, p. 619.

[24] PROKOSHKIN, S. D.—KHMELEVSKAYA, I. Y.—DOBATKIN, S. V.—TRUBITSYNA, I. B.—TATYANIN, E. V.—STOLYAROV, V. V.—PROKOFIEV, E. A.: Acta Mater., *53*, 2005, p. 2703. doi:10.1016/j.actamat.2005.02.032

[25] STOLYAROV, V. V.—GUNDEROV, D. V.—POPOV, A. G.—GAVIKO, V. S.—ERMOLENKO, A. S.: J. Alloys Comp., *281*, 1998, p. 69. doi:10.1016/S0925-8388(98)00774-9

[26] POPOV, A. G. —GAVIKO, V. S.—SHCHEGOLEVA, N. N.—PUZANOVA, T. Z.—ERMOLENKO, A. S.—STOLYAROV, V. V.—GUNDEROV, D. V.—RAAB, G. I.—VALIEV, R. Z.: Phys. Metals Metallogr., *94*, 2002, p. S75.

[27] GAVIKO, V. S.—POPOV, A. G.—ERMOLENKO, A. S.—SHCHEGOLEVA, N. N.—STOLYAROV, V. V.—GUNDEROV, D. V.: Phys. Metals Metallogr., *92*, 2001, p. 158.

[28] DINNEBIER, R. E. [Hrsg.]: Powder Diffraction. Cambridge, RSC Publ. 2008.

[29] SHIMIZU, M.—INOUE, J.: J. Magn. Magn. Mater., *54/57*, 1986, p. 963.

[30] LEVITIN, R. Z.—MARKOSYAN, A. S.—PETROPAVLOVSKII, A. B.—SNEGIREV, V. V.: Phys. Sol. State, *39*, 1997, p. 1633. doi:10.1134/1.1129910

[31] KATTNER, U. R.: JOM, *49*, 1997, p. 14.

[32] VILLARS, P.—CALVERT, L. D.—PEARSON, W. B.: Pearson's Handbook of Crystallographic Data for Intermetallic Phases. Materials Park, Ohio, Amer. Soc. Met. 1996.

[33] JSPDS Database. International Centre for Diffraction Data, 2001.

[34] VALIEV, R. Z.—ISLAMGALIEV, R. K.—ALEXANDROV, I. V.: Progr. Mater. Sci., *45*, 2000, p. 103. doi:10.1016/S0079-6425(99)00007-9

[35] VALIEV, R. Z.—ESTRIN, Y.—HORITA, Z.—LANGDON, T. G.—ZEHETBAUER, M. J.—ZHU, Y. T.: JOM, *58*, 2006, No. 4, p. 33. PMid:10039587

[36] NAZAROV, A. A.—ENIKEEV, N. A.—ROMANOV, A. E.—ORLOVA, T. S.—ALEXANDROV, I. V.—BEYERLEIN, I. J.—VALIEV, R. Z.: Acta Mater., *54*, 2006, p. 985. doi:10.1016/j.actamat.2005.10.025

[37] MASSOBRIO, C.—PONTIKIS, V.—MARTIN, G.: Phys. Rev. Lett., *62*, 1989, p. 1142. doi:10.1103/PhysRevLett.62.1142

[38] MASSOBRIO, C.—PONTIKIS, V.—MARTIN, G.: Phys. Rev., *B 41*, 1990, p. 10486. doi:10.1103/PhysRevB.41.10486

[39] MASSOBRIO, C.—PONTIKIS, V.: Phys. Rev., *B 45*, 1992, p. 2484. doi:10.1103/PhysRevB.45.2484

[40] EVANGELAKIS, G. A.—PONTIKIS, V.: J. Alloys Comp., *483*, 2009, p. 662. doi:10.1016/j.jallcom.2008.07.221

[41] BAKAI, A. S.: Polycluster Amorphous Solids. Moscow, Energoatomizdat 1987 (In Russian).

[42] BAKAI, A. S.: In: Glassy Metals III. Eds.: Beck, H., Guntherodt, H.-J. Heidelberg, Springer 1994, p. 209.

[43] BAKAI, A. S.—BAKAI, S. A.—ECKERT, J.—NEKLYUDOV, I. M.—SAVCHENKO, V. I.: J. Non-Cryst. Solids, *32/40*, 2007, p. 3754. doi:10.1016/j.jnoncrysol.2007.05.142